

Accepted Manuscript

Design and synthesis of potent inhibitors of the mono(ADP-ribosyl)transferase, PARP14

Kristen Upton, Matthew Meyers, Ann-Gerd Thorsell, Tobias Karlberg, Jacob Holechek, Robert Lease, Garrett Schey, Emily Wolf, Adrianna Lucente, Herwig Schüler, Dana Ferraris

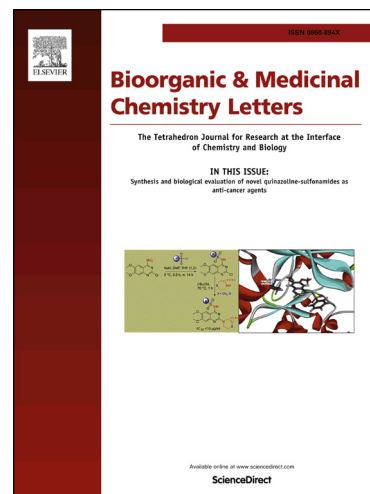
PII: S0960-894X(17)30473-0
DOI: <http://dx.doi.org/10.1016/j.bmcl.2017.04.089>
Reference: BMCL 24942

To appear in: *Bioorganic & Medicinal Chemistry Letters*

Received Date: 28 February 2017
Revised Date: 22 April 2017
Accepted Date: 27 April 2017

Please cite this article as: Upton, K., Meyers, M., Thorsell, A-G., Karlberg, T., Holechek, J., Lease, R., Schey, G., Wolf, E., Lucente, A., Schüler, H., Ferraris, D., Design and synthesis of potent inhibitors of the mono(ADP-ribosyl)transferase, PARP14, *Bioorganic & Medicinal Chemistry Letters* (2017), doi: <http://dx.doi.org/10.1016/j.bmcl.2017.04.089>

This is a PDF file of an unedited manuscript that has been accepted for publication. As a service to our customers we are providing this early version of the manuscript. The manuscript will undergo copyediting, typesetting, and review of the resulting proof before it is published in its final form. Please note that during the production process errors may be discovered which could affect the content, and all legal disclaimers that apply to the journal pertain.



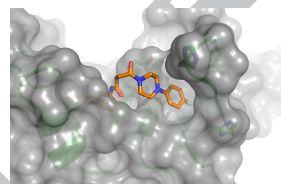
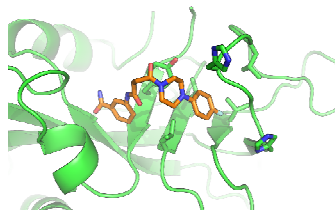
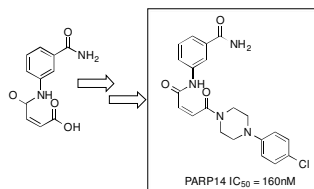
Graphical Abstract

To create your abstract, type over the instructions in the template box below.
Fonts or abstract dimensions should not be changed or altered.

Design and synthesis of potent inhibitors of the mono-(ADP-ribosyl)transferase, PARP14

Leave this area blank for abstract info.

Kristen Upton^a, Matthew Meyers^a, Ann-Gerd Thorsell^b, Tobias Karlberg^b, Jacob Holechek^a, Robert Lease^a, Garrett Schey^a, Emily Wolf^c, Adrianna Lucente^c, Herwig Schuler^b, Dana Ferraris^a





Design and synthesis of potent inhibitors of the mono(ADP-ribosyl)transferase, PARP14

Kristen Upton^a, Matthew Meyers^a, Ann-Gerd Thorsell^b, Tobias Karlberg^b, Jacob Holecek^a, Robert Lease^a, Garrett Schey^a, Emily Wolf^c, Adrianna Lucente^c, Herwig Schüler^b, Dana Ferraris^a

^aMcDaniel College, 2 College Hill, Westminster, MD 21157

^bKarolinska Institutet, Department of Medical Biochemistry and Biophysics, Scheeles väg 2, S-17177 Stockholm, Sweden

^cStevenson University, 1525 Greenspring Valley Rd, Stevenson, MD 21153

ARTICLE INFO

Article history:

Received

Revised

Accepted

Available online

Keywords:

PARP; PARP14; ARTD-8; mono(ADP-ribosyl) transferase

ABSTRACT

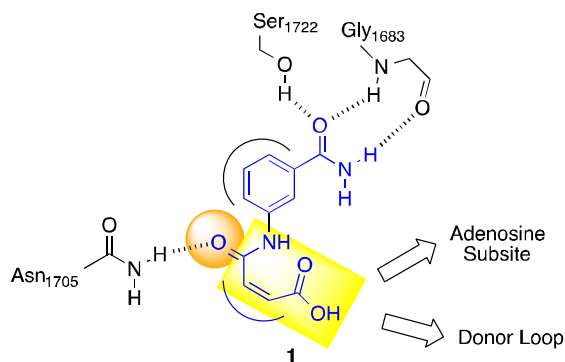
A series of (Z)-4-(3-carbamoylphenylamino)-4-oxobut-2-enyl amides were synthesized and tested for their ability to inhibit the mono-(ADP-ribosyl)transferase, PARP14 (a.k.a. BAL-2; ARTD-8). Two synthetic routes were established for this series and several compounds were identified as sub-micromolar inhibitors of PARP14, the most potent of which was compound **4t**, IC₅₀ = 160nM. Furthermore, profiling other members of this series identified compounds with >20 fold selectivity over PARP5a/TNKS1, and modest selectivity over PARP10, a closely related mono-(ADP-ribosyl)transferase.

2009 Elsevier Ltd. All rights reserved.

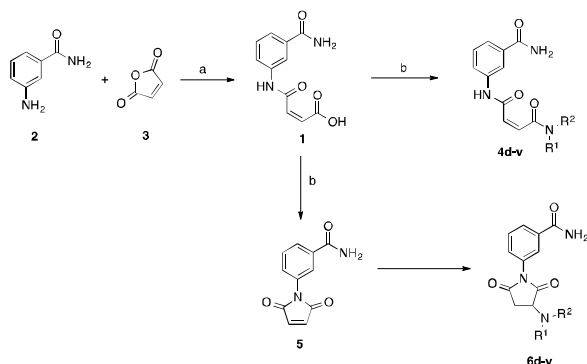
Several members of the Poly-(ADP-Ribose) Polymerase (PARP) family of proteins are attractive targets for oncology-based drug discovery.¹ Much of the research over the past three decades has focused on the inhibition of ADP-ribosyl polymerases PARP-1/2 and tankyrases (PARP 5a/b). However, most other members of the PARP superfamily are mono-ADP-ribosyltransferases, or are catalytically inactive.² Research is branching out toward these PARP family members, but potent and selective tool compounds still do not exist for many of these mono-(ADP-ribosyl)transferases.³ The pharmacological effect of specifically inhibiting these other members of the PARP family is unknown, *thus specific inhibitors or probes must be designed in order to delineate the effects of this inhibition*. One of the members of this family is PARP14 (a.k.a. BAL-2; ARTD-8), a mono-(ADP-ribosyl)transferase. This protein has been demonstrated to have a critical function in the progression of multiple myeloma⁴ and roles in transcription control⁵ and cellular metabolism.⁶ Because of its intriguing therapeutic prospects; PARP14 has been identified as a potential drug discovery target.⁷

Two recent studies focused on identifying small molecule inhibitors of PARP14.^{8,9} These studies identified a low micromolar inhibitor of PARP14 (Z)-4-(3-carbamoylphenylamino)-4-oxobut-2-enoic acid (IC₅₀ = 7-20 μM, Compound **1**, Figure 1) and provided some initial SAR around this compound. This compound represents an ideal starting point for optimization for several reasons: 1) X-ray co-crystal data exists so that the binding mode between **1** and PARP14 is known and iterative structure based design can be used to optimize compounds; 2) Compound **1** is readily synthesized allowing for

rapid generation of a series of analogs; 3) Compound **1** has a low molecular weight (MW = 234) allowing for some growth while still maintaining parameters necessary for a chemical probe;¹⁰ 4) A recent paper described small molecule PARP14 inhibitors with some selectivity over PARP1.¹¹ These inhibitors bridge the nicotinamide and the adenosine subsites. Derivatization of the carboxylate of compound **1** provides an ideal direction to reach the adenosine subsite and possibly the donor loop. Both of these regions have residues unique to PARP14 and could lead to selective PARP14 inhibitors. In the following letter we describe the synthesis and activity of a series analogs derived from **1**. A series of (Z)-4-(3-carbamoyl-phenylamino)-4-oxobut-2-enyl amides was synthesized and compounds **4l** and **4t** represent the most potent derivatives against PARP14 in the literature. While these inhibitors do not demonstrate appreciable selectivity over PARP-1, compounds **4l** and **4r** display ~20 fold selectivity against PARP-5a/5b, and modest selectivity over PARP10. This

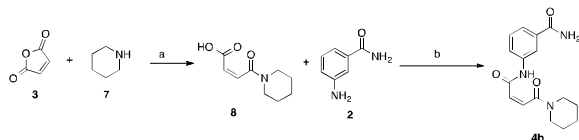


represents a viable starting point toward PARP14 selective inhibitors.



Scheme 1. Reagents and conditions: (a) THF, rt, 83%;⁸ (b) DMF, DIEA, HNR¹R², HATU or TBTU, 10-97%.

Initial SAR on this series⁹ confirmed several important features of the binding mode: 1) the primary amide on the A-ring (blue, Figure 1) forms three hydrogen bonds in the NAD⁺ binding



Scheme 2. Reagents and conditions: (a) THF, 68%; (b) DMF, DIEA, HATU, 45%.

site of PARP14. Thus any derivatization around this amide or replacement of the amide resulted in loss of potency; 2) the double bond of the 4-oxo-2-butenic acid is in a relatively small pocket (yellow box, Figure 1), thus, methylation or replacement of this moiety with large groups or rings resulted in loss of activity; 3) A hydrogen bond exists between Asn1705 and the amide oxygen of the 4-oxobut-2-enoic acid (orange circle, Figure 1), so removal of this amide will most likely result in decreased potency; 4) A relatively large pocket (adenosine binding pocket) exists adjacent to the carboxylate providing an obvious direction for optimization and potential selectivity.¹¹ Many of these interactions are representative of most NAD⁺ competitive PARP-1 inhibitors.¹² This is due to the fact that the PARP family was initially categorized based on homology within the catalytic domain. Despite this homology in the nicotinamide binding site, there are significant differences between the adenosine binding site and the donor loop of PARP14 and that of e.g. PARP1. Recent studies have demonstrated that selectivity can be achieved by targeting the adenosine site,¹¹ and the same has been done for the tankyrases.³ Thus, our strategy for optimization and potential selectivity was to modify this series of compounds with substituents that probe this portion of the enzyme.

The synthesis of (Z)-4-(3-carbamoylphenylamino)-4-oxobut-2-enyl amides **4d-v** is outlined in Scheme 1. The carboxylic acid **1** was synthesized in good yield according to the literature procedure using 3-aminobenzamide **2** and maleic anhydride **3**.⁸ Coupling of compound **1** with secondary amines using HATU or TBTU afforded the amides **4d-v**. Interestingly, minor byproducts were observed under these conditions and characterized as the succinimides **6d-v**. These derivatives presumably arise from the intramolecular cyclization to form the maleimide **5** followed by Michael addition of the amines. In some cases (e.g. piperidine), the Michael addition occurred prior to the coupling resulting in a complicated mixture of products. In order to circumvent the

formation of these byproducts, another route was established as shown in Scheme 2. Piperidine **7** was acetylated with maleic anhydride **3** in THF to afford the intermediate maleic amide **8** in good yield. This amide was coupled with 3-amino benzamide using standard HATU coupling conditions to afford the desired amide **4b**.

Our strategy for developing potent PARP14 inhibitor derivatives consisted of the synthesis of amides from the 4-oxobut-2-enoic acid group. Early attempts at this line of optimization met with little success⁹ as shown by compound **4a** (IC₅₀ = >20μM). Simply replacing the pyrrolidine group with a slightly larger six membered ring such as a piperidine (**4b**, IC₅₀ = 7.7μM) or piperazine (**4c**, IC₅₀ = 11μM) led to two compounds with potency comparable to compound **1** (Table 1). The next logical step towards optimization of this series was to incorporate substituents around each of these rings.

Table 1. Inhibition of PARP14 by 4-oxobut-2-enyl amide derivatives*

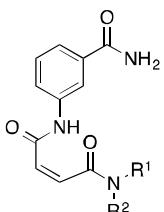
Compd	Structure	PARP14 IC ₅₀ , μM (pIC ₅₀ ±SD, M)	PARP1 IC ₅₀ , μM (pIC ₅₀ ±SD, M)
1		7.6 ⁹	4.4 ⁹
4a		>20 ^a	
4b		7.7 (5.12±0.09)	
4c		11.2 (4.95±0.08)	

*IC₅₀ values for inhibition of PARP14 catalytic fragment by **4b** and **4c** were obtained as described.³

Several 2-, 3- and 4-substituted piperidine derivatives were synthesized and analyzed in vitro as shown by compounds **4d-n** (Table 2). The 2-phenyl (IC₅₀ = 1.1μM) and 2-benzyl (IC₅₀ = 3.5μM) piperidines **4d** and **4e** demonstrated slightly better potency than the parent compound **4b**. Although the 3-substituted ethyl ester **4f** was inactive, notable improvements were also seen with the 3-phenyl analog **4g** (IC₅₀ = 0.69μM) and the 3-phenoxy **4h** (IC₅₀ = 1.4μM) piperidine analogs. While **4g** was the first sub-micromolar derivative in our hands, this analog exhibited very little selectivity against PARP1 (IC₅₀ = 1.6μM) and PARP5a (IC₅₀ = 2.7μM). Similar to the 3-substituted ester, the 4-substituted ester derivative **4i** did not demonstrate appreciable potency against PARP14. Homologation of this ester led to a definite improvement in activity as shown by compound **4j** (IC₅₀ = 2.4μM). The 4-phenylpiperidine derivative **4k** demonstrated low micromolar activity, (IC₅₀ = 2.2μM), but interestingly the

addition of an electron withdrawing fluorine atom led to compound that was approximately 10x more potent (**4l**, $IC_{50} = 0.27\mu M$). Addition of a carbon between the piperidine and aromatic ring also seemed to improve potency leading to another sub-micromolar derivative (**4m**, $IC_{50} = 0.45\mu M$). More importantly compounds **4l** and **4m** demonstrated notable improvements in selectivity over PARP5a. Compound **4l** was ~30 fold selective and compound **4m** was ~11 fold selective over PARP5a. Compound **4l** was also ~10 fold selective over the mono-ADP-ribosyltransferase, PARP10. Unfortunately, the most potent derivatives of this series were nearly all equipotent against PARP1, but these data were encouraging and prompted the synthesis of structurally similar N-aryl piperazines to potentially improve the potency and selectivity.

Table 2. Inhibition data by piperidinyl-amide derivatives*

#	-NR ¹ R ²			
		PARP14 IC_{50} μM (p $IC_{50} \pm SD$, M)	PARP1 IC_{50} μM (p $IC_{50} \pm SD$, M)	PARP5a IC_{50} μM (p $IC_{50} \pm SD$, M)
4d		1.1 (5.97±0.14)		
4e		3.5 (5.45±0.07)		
4f		21% @ 5 μM		
4g		0.69 (6.16±0.09)	1.6 (5.81±0.3)	2.7 (6.24±0.1)
4h		1.4 (5.99±0.13)	90% @ 5 μM	
4i		28% @ 5 μM		
4j		2.4 (6.39±0.15)		
4k		2.2 (5.65±0.08)		
4l		0.27 (6.56±0.09)	0.27 (6.56±0.1)	8.0 (5.1±0.09)
4m		0.45 (6.35±0.07)	0.23 (6.63±0.06)	4.8 (5.32±0.07)
4n		0.65 (6.17±0.07)		

* IC_{50} values for inhibition of full length PARP1 and PARP14 and PARP5a catalytic fragments were obtained as described.³

The inhibitory potency of these piperazine derivatives is detailed in Table 3. While the core piperazine derivative **4c** displayed relatively modest potency (**4c**, $IC_{50} = 11\mu M$), the t-butoxy carbonyl derivative **4o** ($IC_{50} = 0.37\mu M$) demonstrated a notable improvement. Improvements in potency were also noted by incorporation of an aryl ring onto the piperazine nitrogen. Compounds **4p**, **4r**, **4s** and **4t** all displayed potency below $1\mu M$. In fact, **4t** ($IC_{50} = 160nM$) is almost an order of magnitude more potent than the parent **4c** and represents one of the most potent PARP14 inhibitors in the literature. Addition of another aromatic ring as demonstrated by the biphenyl derivative **4q** ($IC_{50} = 4.2\mu M$) was not as effective as just one aryl ring. Similarly, incorporation of a heteroaryl group onto the piperazine (**4v**, $IC_{50} = 2.8\mu M$), was also detrimental to inhibitory potency as was the addition of an electron donating methoxy group on the aromatic ring (**4u**, $IC_{50} = 3.4\mu M$). The succinimide byproduct, **6r**, of one of the most potent aryl piperazine analogs, **4r**, was completely inactive (PARP14 $IC_{50} > 20\mu M$). Unfortunately, the most potent derivatives in this sub-series (i.e. **4p**, **4r**, **4s** and **4t**) displayed a relative lack of selectivity against PARP1, but these analogs still maintained reasonable selectivity over PARP5a (**4p** = 6.7 fold, **4r** = 23 fold, **4s** = 3.9 fold, **4t** = 5.6 fold) and PARP10 (**4r** = 7.8 fold, **4s** = 6.1 fold). We also measured the inhibition of several other mono-ADP-ribosyltransferases by **4s** (IC_{50} values: PARP12, 8.2 μM ; PARP15, 0.52 μM ; PARP16, 0.56 μM).

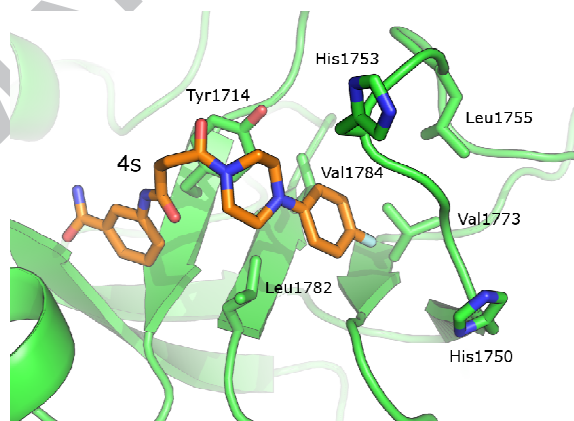
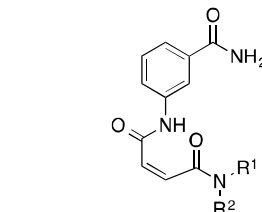


Figure 2. Crystal structure of 4s bound to the catalytic domain of PARP14. Protein sidechains discussed in the text are indicated. Protein Data Bank entry 5NQE.

A crystal structure of the catalytic domain of PARP14 in complex with **4s** can illustrate what we believe to be the general binding mode of the more potent derivatives of the scaffold examined here (Figure 2). As expected, the aminobenzamide moiety is bound in the nicotinamide pocket in a conformation very similar to the vast majority of PARP inhibitors, which occupy that site. The oxybutenyl linker is within hydrogen bonding distance of the Tyr1721 hydroxyl. However, the flexibility of the linker allows the distal fluorinated aryl ring of **4s** to reside in a hydrophobic environment created by the Leu1755, Val1773, and Val1784 side chains as well as Leu1782, the small hydrophobic residue that replaces the catalytic glutamate of PARP1. Our binding data indicate that the piperazine ring has a conformation that is slightly better suited to accommodate these hydrophobic interactions, as compared to the piperidine. Together, these results suggest that a number of chemistry strategies remain to achieve more potent inhibition of PARP14: The hydrophobic interaction site of **4s** is delimited by an aromatic amino acid (Tyr1714), with π - π stacking/interactions

potential, as well as by His1750 and His1753. Furthermore, the D-loop is apparently flexible and can adopt to a number of ligand induced conformations.^{3,8,9,11} Since this loop is relatively variable among PARP family members, engagement of a non-conserved D-loop side chain remains a promising strategy toward a potent and selective mono-(ADP-ribosyl)transferase inhibitor.

Table 3. Inhibition data by piperazinyl-amide derivatives*

#	-NR ¹ R ²	PARP14 IC ₅₀ (μM) (pIC ₅₀ ±SD, M)	PARP1 IC ₅₀ (μM) (pIC ₅₀ ±SD, M)	PARP5a IC ₅₀ (μM) (pIC ₅₀ ±SD, M)
4o		0.37 (6.43±0.09)		

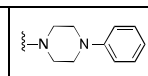
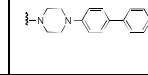
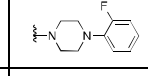
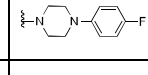
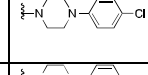
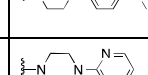
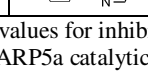
In conclusion we outline the synthesis and activity of several of the most potent inhibitors of PARP14 described. Despite the lack of selectivity against PARP-1 several analogs in this series display >10 fold selectivity over PARP5a and >5 fold selectivity over closely related PARP10 (**4r** = 7.8 fold, **4s** = 6.1 fold). Future work will focus on achieving selectivity over PARP-1 by improving interactions between the amide side chains and the D-loop of PARP14.

Acknowledgments

Special appreciation goes to the Johns Hopkins University Drug Discovery group, McDaniel College Chemistry Department, McDaniel College Student Faculty Research Fund, Student Research and Creativity Grant, and Dr. Garry Smith at the Fox Chase Cancer Center for generous support. H.S. received funding from the Swedish Cancer Society (2014/716), the Swedish Research Council (2015-04603), and the IngaBritt and Arne Lundbergs Research Foundation (no. 403). We thank the Protein Science Facility at Karolinska Institutet/SciLifeLab and the beamline staff at the Diamond Light Source (Didcot, UK) for excellent support. Synchrotron data collection was supported by the European Community's Seventh Framework Programme (FP7) under BioStruct-X (no. 283570).

References and notes

1. Curtin, N. J., Sharma, R. A. eds. *PARP Inhibitors for Cancer Therapy*, Springer International Press, Switzerland, 2015.

4p		0.9 (6.05±0.11)	0.37 (6.44±0.15)	6.0 (5.2±0.08)
4q		4.2 (5.38±0.2)	0.8 (6.09±0.09)	9.8 (5.01±0.08)
4r		0.41 (6.39±0.1)	0.51 (6.3±0.11)	9.4 (5.03±0.06)
4s		0.70 (6.15±0.07)	0.56 (6.25±0.04)	2.7 (5.57±0.28)
4t		0.16 (6.21±0.16)	0.22 (6.65±0.04)	0.9 (6.01±0.13)
4u		3.4 (5.47±0.11)		
4v		2.8 (5.55±0.1)		

*IC₅₀ values for inhibition of full length PARP1 and PARP14 and PARP5a catalytic fragments were obtained as described.³

2. Hottinger, M. O.; Hassa, P. O.; Lüscher, B.; Schüler, H.; Koch-Nolte, F.; *Trends Biochem. Sci.*, **2010**, *35*, 208-219.
3. Thorsell, A.-G.; Ekblad, T.; Karlberg, T.; Löw, M.; Pinto, A.F.; Trésaugues, L.; Moche, M.; Cohen, M.S.; Schüler H. *J. Med. Chem.* **2017**, *60*, 1262-1271.
4. Barbarulo A.; Iansante V.; Chaidos A.; Naresh K.; Rahemtulla A.; Franzoso G.; Karadimitris A.; Haskard D. O.; Papa S.; Bubici C., *Oncogene* **2013**, *32*, 4231-4242.
5. Mehrotra P.; Riley R.; Patel F.; Li L.; Voss S.; Goenka S., *J. Biol. Chem.* **2011**, *286*, 1767-1776.
6. Iansante V.; Choy P. M.; Fung S. W.; Liu Y.; Chai J.-G.; Dyson J.; Del Rio A.; D'Santos C.; Williams R.; Chokshi S.; Anders R. A.; Bubici C., *Nature Comm.* **2015**, *6*:7882 | DOI: 10.1038/ncomms8882.
7. Camicia R.; Winkler H. C.; Hassa P. O., *Mol. Cancer* **2015**, *14*, 1-62.
8. Andersson, C. D.; Karlberg, T.; Ekblad, T.; Lindgren, A. E. G.; Thorsell, A.-G.; Spjut, S.; Uciechowska, U.; Niemiec, M. S.; Wittung-Stafshede, P.; Weigelt, J.; Elofsson, M.; Schüler, H.; Linusson, A., *J. Med. Chem.* **2012**, *55*, 7706-7718.
9. Ekblad, T.; Lindgren, A. E. G.; Andersson, C. D.; Caraballo, R.; Thorsell, A.-G.; Karlberg, T.; Spjut, S.; Linusson, A.; Schüler, H.; Elofsson, M. *Eur. J. Med. Chem.* **2015**, *95*, 546-551.
10. Frye, S. V., *Nature Chem. Biol.* **2010**, *6*, 159-161.
11. Peng, B.; Thorsell, A.-G.; Karlberg, T.; Schüler, H.; Yao, S. Q., *Angew. Chem. Int. Ed.* **2016**, *55*, 1-7.
12. Ferraris, D. *J. Med. Chem.* **2010**, *53*, 4561-4584.

Supplementary data

Supplementary data contains experimental procedures, enzyme purification and enzymatic assay details. These data can be found online.